crystallization communications

Crystallization and preliminary X-ray analysis of the isomerase domain of glucosamine-6-phosphate synthase from *Candida albicans*

Jaroslaw Olchowy,[a] Robert Jedrzejczak,[b] Slawomir Milewski[a] and Wojciech Rypniewski[c]*

[a]Department of Pharmaceutical Technology and Biochemistry, Gdansk University of Technology, ul. Narutowicza 11/12, 80-952 Gdansk, Poland, [b]Argonne National Laboratory, Biosciences Division, 9700 South Cass Avenue, Argonne, IL 60439, USA, and [c]Institute of Bioorganic Chemistry, Polish Academy of Sciences, ul. Noskowskiego 12/14, 61-704 Poznan, Poland

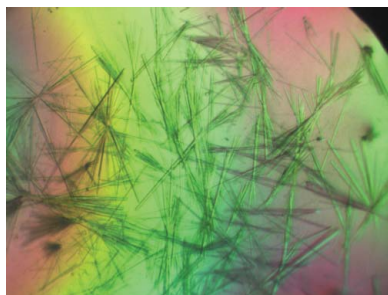Correspondence e-mail: wojtekr@ibch.poznan.pl

Glucosamine-6-phosphate synthase (EC 2.6.1.16) catalyses the first and practically irreversible step in the hexosamine metabolism pathway, the end product of which, uridine 5′-diphospho-*N*-acetyl D-glucosamine, is an essential substrate for assembly of the cell wall. The isomerase domain, consisting of residues 346–712 (42 kDa), of glucosamine-6-phosphate synthase from *Candida albicans* has been crystallized. X-ray analysis revealed that the crystals belonged to space group $I4$, with unit-cell parameters $a = b = 149$, $c = 103$ Å. Diffraction data were collected to 3.8 Å. Preliminary results from molecular replacement using the homologous bacterial monomer reveal that the asymmetric unit contains two monomers that resemble a bacterial dimer. The crystal lattice consists of pairs of such symmetry-related dimers forming elongated tetramers.

1. Introduction

Glucosamine-6-phosphate synthase (L-glutamine:D-fructose-6-phosphate amidotransferase; EC 2.6.1.16) catalyses the first and practically irreversible step in the hexosamine-metabolism pathway, a branch of the glycolytic pathway (reviewed by Milewski, 2002). The end product of the hexosamine-metabolism pathway is uridine 5′-diphospho-*N*-acetyl-D-glucosamine (UDP-GlcNAc), an essential substrate for assembly of the cell wall in fungi and bacteria. Fungal glucosamine-6-phosphate (GlcN-6-P) synthase is of interest as a potential target in antifungal therapy and is part of our wider study aimed at improved chemotherapy against fungal pathogens by targeting their vital functions. Conditions favouring fungal pathogens occur ever more frequently as an unintentional result of the use of antibiotics or in the course of diseases that weaken the human immune system. Fungi, being eukaryotes like the organisms they infect, present a subtler challenge to medicine than bacteria. The enzyme under study in this project comes from the fungus *Candida albicans*, an opportunistic human pathogen classified as a yeast. Although there is a clear amino-acid sequence homology between the bacterial and yeast GlcN-6-P synthases, the enzyme architecture is more complex in eukaryotes than in prokaryotes. In *Escherichia coli* the protein is a homodimer of subunit molecular weight ∼70 kDa, while the eukaryotic protein is a homotetramer of 80 kDa subunits (Milewski *et al.*, 1999). In addition, only the eukaryotic enzyme is allosterically inhibited by UDP-GlcNAc, the end product of the reaction pathway. The reaction mechanism of GlcN-6-P synthase, both prokaryotic and eukaryotic, is complex and involves amino transfer and sugar isomerization. X-ray crystallographic studies of prokaryotic GlcN-6-P synthase revealed that these two functions were performed by two distinct structural domains of the enzyme subunit (Isupov *et al.*, 1996; Teplyakov *et al.*, 1999, 2001). The isomerase domain is believed to be responsible for oligomerization of the *C. albicans* GlcN-6-P synthase (Milewski, unpublished data). For the purpose of these studies, we constructed and purified a recombinant protein comprising residues 346–712 of the native *C. albicans* GlcN-6-P synthase (Olchowy *et al.*, 2004). This fragment demonstrated a very high degree of homology to the 241–608 part of the *E. coli* enzyme, unequivocally identified as its isomerase domain (Teplyakov *et al.*, 1998). Here, we report the crystallization and

Table 1
Data-collection statistics.

Values in parentheses are for the last resolution shell.

Beamline	EMBL-X11
Temperature (K)	100
Wavelength (Å)	0.8128
Space group	$I4$
Unit-cell parameters (Å)	
$\quad a = b$	149.3
$\quad c$	103.0
Resolution range (Å)	20.0–3.8 (3.87–3.80)
R_{merge}†	0.132 (0.308)
No. of raw measurements	230399
No. of unique reflections	11183
Completeness (%)	100.0 (100.0)
Mosaicity (°)	0.5
Data redundancy	4.4 (4.6)
$\langle I/\sigma(I)\rangle$	11.5 (5.4)
Reflections > 3σ (%)	76 (62)

† $R_{merge} = \sum |I - \langle I \rangle| / \sum I$, where $\langle I \rangle$ is the average intensity for a given measurement and the summation is over all measurements

preliminary X-ray analysis of the isomerase domain of GlcN-6-P synthase from *C. albicans*.

2. Methods and results

2.1. Expression and purification

The His$_6$-N-tagged isomerase domain of GlcN-6-P synthase was overproduced in *E. coli* BL21(DE3)pLysS cells transformed with the pET23b-FRU expression plasmid. Overexpression was induced with isopropyl-β-D-thiogalactopyranoside at a final concentration of 0.5 mM. The overproduced protein was isolated in a three-step procedure involving preparation of crude extract, metal-chelate affinity chromatography performed on Ni^{2+}-IDA agarose (His-Bind Resin, Novagen) and gel filtration on Superdex 200 (Olchowy *et al.*, 2004). The protein was isolated with 81% yield. The purified protein was stored and crystallized from an aqueous solution containing 10 mM HEPES pH 7.0, 10 mM glucose-6-phosphate (Glc-6-P) and 10 mg ml^{-1} protein.

2.2. Crystallization

Numerous attempts to crystallize the protein failed using several commercial crystallization kits as well as home-made mixtures of commonly used salts and organic solvents. Finally, we obtained crystals using Clear Strategy Screen 1 (Molecular Dimensions). Thin needle-shaped crystals grew as hanging drops or sitting drops in
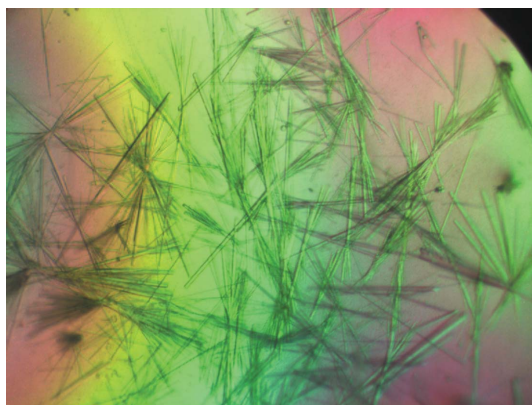
Figure 1
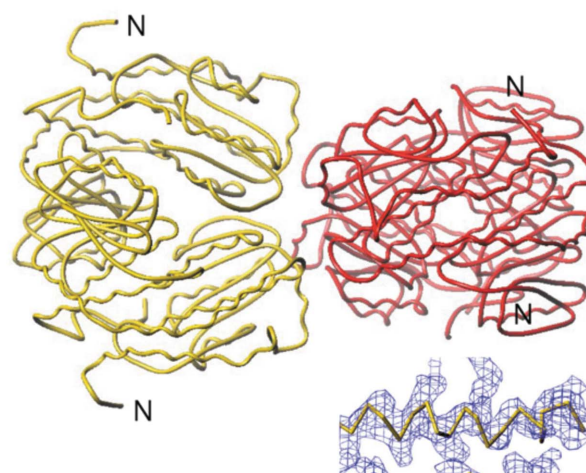Crystals of the isomerase domain of GlcN-6-P synthase

vapour-diffusion setups in 20%(w/v) PEG 600 and 0.15 M KSCN at pH 8.5 (Fig. 1). Several other solutions in the kit, all containing KSCN, also gave small crystals. The crystals grew at 277 K and dissolved slowly at room temperature. The needles grew up to 0.3 mm in length, but their thickness was limited to ∼20 µm.

2.3. Data collection and analysis

X-ray diffraction data were collected at the EMBL X11 beamline at the DORIS storage ring, DESY, Hamburg from a crystal of the isomerase domain grown in the presence of Glc-6-P. The thin needle-shaped crystals were very fragile and difficult to handle; they were also difficult to cryocool. Transferring the crystals to solutions containing any of the commonly used cryoprotectants invariably caused a major loss of X-ray diffraction. The crystals could be vitrified successfully only if oil was used for cryoprotection. Light oils with low viscosity generally gave better results than heavy oils. The best turned out to be 'Iliada' Greek salad oil (Agrovim). Diffraction images were recorded on a MAR CCD 165 mm detector and processed with the *DENZO/SCALEPACK* program suite (Otwinowski & Minor, 1997). Data statistics are summarized in Table 1. The space group was determined to be $I4$ based on autoindexing of the diffraction spots, merging the data assuming different symmetries and analysis of the systematic absences (none were found). The V_M value assuming two monomers per asymmetric unit was 3.4 Å^3 Da^{-1}, corresponding to a solvent content of 64% (Matthews, 1968).

2.4. Molecular replacement

The phase problem was solved by molecular replacement using the program *PHASER* v.1.3 running in automatic mode (McCoy *et al.*, 2005) using as the search model the atomic coordinates (all protein atoms) of the isomerase domain from the GlcN-6-P synthase from *E. coli* (PDB code 1moq; Teplyakov *et al.*, 1998). The rotation function contained three peaks higher than 75% of the difference between the top and the mean value. The peaks were at 4.2, 4.1 and 3.4 standard deviations above the mean (Z scores). After the trans-

Figure 2
A tetramer of isomerase domains of the GlcN-6-P synthase obtained as the result of molecular replacement performed with the homologous domain of the *E. coli* synthase (Teplyakov *et al.*, 1998) as the search model. The monomers associate pairwise, as in the bacterial dimer. Two such symmetry-related dimers (shown in different colours) associate back-to-back in the *C. albicans* crystal structure. The N-termini of the polypeptide chains are indicated. The inset in the bottom right corner shows an α-helical fragment of the electron density after the density-modification procedure, as described in the text. The map was contoured at the level of one root-mean-square deviation.

lation function, the first two peaks (corresponding to the first two peaks of the rotation function) had Z scores of 14 and 16, respectively, with no steric clashes. The remaining peaks in the translation function had Z scores near 5. Although a single subunit was used as the search model, the solution obtained from molecular replacement consisted of two subunits interacting in a similar way to subunits in the bacterial dimer. The crystal lattice consisted of symmetry-related pairs of such dimers interacting end-to-end (Fig. 2). The phases obtained from molecular replacement were used in an electron-density modification procedure that included non-crystallographic symmetry averaging, solvent flattening and histogram matching using the program *DM* (Cowtan, 1994). The molecular envelope was determined using the automatic protocol of *DM* with the solvent content set at 60%. The NCS correlation between the related symmetry regions was initially 0.82 and increased to 0.97 after 100 cycles of averaging while increasing the resolution from 8.0 to 3.8 Å. The electron-density map thus obtained shows a significant improvement and departure from the initial map based on molecular replacement. The map shows interpretable density (inset in Fig. 2) for most of the protein and good surface complementarity between the pairs of subunits that form the tetramer.

3. Discussion

The crystals are small and difficult to handle. Nevertheless, useful X-ray data were obtained. Despite the weak intensities and limited resolution of the data, the phase problem has been solved unambiguously and the initial electron-density map is interpretable. Much remains to be done before an atomic model is fully built and refined, but the results obtained already reveal the basic plan of the oligomeric structure of the isomerase domains in the *C. albicans* GlcN-6-P synthase. In prokaryotes, the isomerase domains form the core of the dimeric molecule. It is likely that in the eukaryotic enzyme the isomerase domains also form the core of the tetrameric molecule. The monomers in the crystal lattice interact in such a manner that their N-termini point outwards. It is possible that in the intact synthase molecule the glutaminase domains that form the N-terminal part of the polypeptide chains also point outward.

When the model of atomic coordinates is built and refined it should enable us to compare the isomerase domain of the eukaryotic GlcN-6-P synthase with the related prokaryotic protein. Of particular interest are the differences that account in eukaryotes for the additional binding site of the allosteric effector UDP-GlcNAc. This compound is known to inhibit eukaryotic but not prokaryotic GlcN-6-P synthase (Milewski, 2002) and our preliminary data indicate that in the *C. albicans* enzyme the UDP-GlcNAc binding site is located in the isomerase domain. This domain contains also the binding site for transition-state analogue inhibitors such as 2-amino-2-deoxy-D-glucitol 6-phosphate (Badet-Denisot *et al.*, 1995), its derivatives (Bearne & Blouin, 2000; Janiak *et al.*, 2003) and arabinose-5-phosphate oxime (Le Camus *et al.*, 1998). We hope that structural analysis of the fungal enzyme will facilitate designing antifungal drugs, allow a deeper understanding of the key metabolic processes of amino-sugar biosynthesis in fungi and elucidate aspects of evolution of major enzymes involved in these processes.

References

Badet-Denisot, M.-A., Leriche, C., Massiere, F. & Badet, B. (1995). *Bioorg. Med. Chem. Lett.* **5**, 815–820.

Bearne, S. L. & Blouin, C. (2000). *J. Biol. Chem.* **275**, 135–140.

Cowtan, K. (1994). *Jnt CCP4/ESF–EACBM Newsl Protein Crystallogr.* **31**, 34–38.

Isupov, M. N., Obmolova, G., Butterworth, S., Badet-Denisot, M. A., Badet, B., Polikarpov, I., Littlechild, J. A. & Teplyakov, A. (1996). *Structure*, **4**, 801–810.

Janiak, A. M., Hoffmann, M., Milewska, M. J. & Milewski, S. (2003). *Bioorg. Med. Chem.* **11**, 1653–1662.

Le Camus, C., Badet-Denisot, M.-A. & Badet, B. (1998). *Tetrahedron Lett.* **39**, 2571–2572.

McCoy, A. J., Grosse-Kunstleve, R. W., Storoni, L. C. & Read, R. J. (2005). *Acta Cryst.* D**61**, 458–464.

Matthews, B. W. (1968). *J. Mol. Biol.* **33**, 491–497.

Milewski, S. (2002). *Biochim. Biophys. Acta*, **1597**, 173–192.

Milewski, S., Kuszczak, D., Jedrzejczak, R., Smith, R. J., Brown, A. J. & Gooday, G. W. (1999). *J. Biol. Chem.* **274**, 4000–4008.

Olchowy, J., Sachadyn, P., Kur, J. & Milewski, S. (2004). *Eur. J. Biochem.* **271**, Suppl. 1, P.32-38.

Otwinowski, Z. & Minor, W. (1997). *Methods Enzymol.* **276**, 307–326.

Teplyakov, A., Obmolova, G., Badet, B. & Badet-Denisot, M. A. (2001). *J. Mol. Biol.* **313**, 1093–1102.

Teplyakov, A., Obmolova, G., Badet-Denisot, M. A. & Badet, B. (1999). *Protein Sci.* **8**, 596–602.

Teplyakov, A., Obmolova, G., Badet-Denisot, M. A., Badet, B. & Polikarpov, I. (1998). *Structure*, **15**, 1047–1055.